The Iraqi Journal For Mechanical And Material Engineering, Vol.13, No3, 2013

AERODYNAMIC AND STRESS ANALYSIS OF A MANNED AIRCRAFT WING (NACA 4412 AIRFOIL)

Adil A. AL-Moosawy Qasim H. Bader Ahmed R. Madeh

ABSTRACT

This research involved a study of aerodynamic analysis to determine the load on a wing of a manned aircraft using ANSYS[11] software program. Awing of aircraft at Mach number (M=0.4) has been modeled in this program to determine the pressure distribution on both wing sides for steady and unsteady states. The wing has been tested at three angles of attack, namely (0° , 5°, 10°). The pressure distribution on the wing has been used to evaluate the stress distribution and displacement for the wing structure. The stress analysis has been carried out for the skin shell of the wing and the internal stiffeners of the wing box. The result obtained in the present work showed that the maximum Von Misses stress occurs at distance of 0-15% from the edge of wing, especially at the **corners** at which spars web extending from the wing and root ribs intersects the wing skin.

ألتحليل الديناميكي الهوائي وتحليل الأجهاد لجناح طائرة مسيرة
(NACA 4412 AIRFOIL)

الخلاصة

تضمن هذا البحث دراسة التحليل الديناميكي الهوائي لأيجاد توزيع الظغط على جناح طائرة مسيرة بأستخدام برنامج (ANSYS[11]) ، تم بناء الموديل الرياضي باستخدام هذا البرنامج عند سرعة (M=0.4) لأيجاد توزيع الضغوط على كل من سطحي الجناح الأعلى والأسفل. الجناح تم أختباره لثلاث زوايا طيران (angle of attack) هي (0°, 5°, 10°) ولكل من الحالتين المستقرة (steady state) والغير مستقرة (unsteady state). الضغط المستخرج من هذه الخطوة أستخدم لأيجاد توزيع الأجهاد والأزاحة على القشرة الخارجية للجناح وكذلك التراكيب الداخلية المقوية للجناح. وجد أن أعظم قيمة للأجهاد تقع في المنطقة (0-15%) من الحافة المثبتة عند جذر الجناح وخصوصا في الزوايا التي تتقاطع فيها سارية الجناح مع الأضلاع وقشرة الجناح.

NOMENCLATURE

Symbol	description	unit
C	Speed of sound in fluid medium	m/s
P	Acoustic pressure P (x,y,t)	N / m^2
T	Time	Sec.
ρ	Density	kg / m^3
$\{n\}$	Unit normal to the fluid-structure interface	---
$\{N\}$	Element shape function for pressure	---
$\{N\}'$	Element shape function for displacement	---
P_e	Nodal pressure vector	N / m^2
u_e	Nodal displacement component vectors	m
M_e^p	Fluid mass matrix	kg
K_e^p	Fluid stiffness matrix	$N/$m
σ_i	Normal stress in i-direction	N / m^2
ε_i	Normal strain in i-direction	---
C_{ij}	Element of elasticity matrix to material axis	N / m^2
α	Angle of attack	degree

1. INTRODUCTION

For structural analysis of a wing, it is necessary to find the loading on the wing. This loading is due to aerodynamic forces coming from 3D pressure distribution on the wing. The distribution of these aerodynamic forces acting on the wing can be found by a numerical methods using CFD analysis. In this study, CFD method is used to calculate the flow field around the wing and the resulting 3D pressure distribution acting on the wing. Then from this pressure distribution, the nodal forces are calculated and then they are exported into the finite element program. In this study, flow field computations are performed using the commercially available CFD tool and the structural analyses were performed by ANSYS[11] software program.

Insuyu, (2010), aimed to increase the aerodynamic efficiency of the aerial vehicles is examined. Among different alternatives, the methodology of increasing the aerodynamic efficiency is chosen as change in camber. The background of the study is established by performing 2D CFD analyses on differently cambered airfoils generated from the selected NACA4412 airfoil via ANSYS®/FLUENT software.

Abid-Aun, (2008), studied the static analysis of the wing by ANSYS package has been presented and used to determine the stress distribution on the wing. This operation involve using the CFD method to obtain the aerodynamic result at (M=0.7) for taper wing and (M=0.2) for rectangle wing. This aerodynamic result (pressure) is used to simulate the wing loading on the wings during the static analysis also using isotropic in design the parts of wing.

Soysal, (2008), Determined the structural analysis of unmanned aerial vehicle wing. Aerodynamic loading around the wing is found via CFD analysis and at the end of the CFD analysis, the nodal forces on the wing surface mesh are transferred to FEA mesh via interpolation. The structural analysis of the unmanned aerial vehicle wing is performed. Linear static analysis of the wing is performed at two different loading conditions which are positive high angle of attack and positive low angle of attack.

Sakarya and Evren, (2010), presents a camber morphing concept as an alternative to existing plain flap aileron type hinged control surface used in wings. Structural aspect of the concept is investigated with static nonlinear finite element analysis by using MSC NASTRAN .In order to assess the aerodynamic characteristics; CFD based 2D solution is obtain using ANSYS Fluent package.

In the present work, it has been concentrated in calculate the aerodynamic load analysis and produced pressure distribution on the wing for study and unsteady state with different angle of attack. Stress distribution on the wing and internal structures of the wing (ribs and spars) was performed for static analysis**.**

2. MATHEMATICAL MODEL

2.1. Governing Equation

The structural dynamics equation need to be considered along with the Navier-Stokes equation .The discretized structural dynamic equation can be formulated using the structural elements are simplified to get the acoustic wave equation using following assumption that was detailed by Unlusoy (2010).

1-The fluid is compressible.

2-The fluid is inviscid (no viscous dissipation).

3-there is no mean flow of the fluid.

4-The mean density and pressure are uniform throughout the fluid.

The acoustical wave equation describes the variation of pressure p with time and space in two dimension Cartesian coordinates (x, y). The acoustic wave equation for two dimensions (unit thickness) is given by:

$$\frac{\partial^2 P}{\partial^2 x}+\frac{\partial^2 P}{\partial^2 y}=\frac{1}{c^2}\frac{\partial^2 P}{\partial^2 t} \quad (1)$$

Boundary

condition: $P(x,y,t)=\overline{P}\,e^{i\omega t}$ (2)

Initial condition (t=0): $P(x,y,0)=\overline{P}$

Then equation (1) reduced to the Helmholtz equation Erdogan (2010):

$$\frac{\omega^2\overline{P}}{c^2}+\left(\frac{\partial^2}{\partial^2 x}+\frac{\partial^2}{\partial^2 y}\right)\overline{P}=0 \quad (3)$$

Then, the finite element statement of the wave equation (1) is given by:

$$\int_{vol}\frac{1}{c^2}\{\delta P_e\}^T\{N\}\{N\}^T\,d(vol)\{\ddot{P}_e\}+\int_{vol}\{\delta P_e\}^T[B]^T[B]\,d(vol)\{P_e\}$$
$$+\int_S \rho_o\{\delta P_e\}^T\{N\}\{n\}^T\{N'\}^T\,d(S)\{\ddot{u}_e\}$$
$$=\{0\} \quad (4)$$

Equation (4) can be written in matrix notation to get the discretized wave equation:

$$[M_e^P]\{\ddot{P}_e\}+[K_e^P]\{P_e\}+\rho_o[R_e]^T\{\ddot{u}_e\}=\{0\} \quad (5)$$

Pressure distribution across the upper and lower surface was calculated for transient flow through time (0.2 second) with time increment (Δt=0.02 second) by using ANSYS[11] package.

3. STRESS ANALYSIS

A static analysis calculates the effects of steady and unsteady state pressure condition which applied on the element of a structure at the upper and lower surface. The wing of structure is subjected to static element pressure load. Preliminary design of this structure against those loads is assumed from the Aluminum 7075-T651, Soysal (2008). The results of the static analysis would be included the element stresses distribution on the wing structure and the internal structure which included the ribs and spars along element coordinates axis, the linear and angular displacements of the nodes $(u, v, w, \theta_{xi}, \theta_{yi}, \theta_{zi})$ along global coordinate axis.

When performing analysis by displacement based finite elements a way to relate stresses to the determined displacement and thus strains is needed. By applying the assumption of linear elastic material behavior the constitutive law, known as Hooke's generalized law provides the sought relation. Hansen and Hvejsel,(2006).

$$\sigma = C\varepsilon \quad (6)$$

Here the stresses σ are related to strains ε in a linear manner through the constitutive matrix C (6×6). Exploiting symmetry conditions and making strain energy considerations it can be shown that only 21 constants are needed in the description of anisotropic materials.

$$\begin{Bmatrix} \sigma_x \\ \sigma_y \\ \sigma_z \\ \tau_{xy} \\ \tau_{yz} \\ \tau_{xz} \end{Bmatrix} = \begin{bmatrix} C_{11} & C_{12} & C_{13} & C_{14} & C_{15} & C_{16} \\ C_{21} & C_{22} & C_{23} & C_{24} & C_{25} & C_{26} \\ C_{31} & C_{32} & C_{33} & C_{34} & C_{35} & C_{36} \\ C_{41} & C_{42} & C_{43} & C_{44} & C_{45} & C_{46} \\ C_{51} & C_{52} & C_{53} & C_{54} & C_{55} & C_{56} \\ C_{61} & C_{62} & C_{63} & C_{64} & C_{65} & C_{66} \end{bmatrix} \begin{Bmatrix} \varepsilon_x \\ \varepsilon_y \\ \varepsilon_z \\ \gamma_{xy} \\ \gamma_{yz} \\ \gamma_{xz} \end{Bmatrix} \tag{7}$$

4. MAIN CHARACTERISTICS OF THE WING

4.1 Aircraft wing geometric parameters

The basic parameter such as airfoil section, wing plane form S, wing chord length C, wing span B, aspect ratio A, tapered ratio λ and thickness to chord ratio t/c should have been decided at early stages of the work .Table (1) shows details of these parameters for the wing in this study, and figure (1) shows airfoil NACA 4412 of the wing selected in the present study.

4.2 Materials

Historically, aluminum materials have been the primary material for aircraft and space craft construction. Today, structural weight and stiffness requirements have exceeded the capability of conventional aluminum, and high-performance payloads have demanded extreme thermo-elastic stability in the aircraft design environment.

4.3 Element types

The most commonly used element type in aerospace industry is the two-dimensional (2D) elements since the industry is mostly dealing with thin walled structures. Almost every main structural part can be modeled using these types of elements. While three dimensional (3D) type elements are not performed for aerospace application.

5. RESULTS AND DISCUSSIONS

5.1 Aerodynamic Analysis

In this work the aerodynamic load was calculated by using ANSYS^{11} ○ software for the representative wing section (airfoil) as 2D in wind tunnel for NACA 4412 with different angles of attack.

Fig.2 to Fig.4 demonstrate the contour map of pressure distribution over two dimension airfoil NACA 4412 with different angles of attack $\alpha = 0°, \alpha = 5°$ and $, \alpha = 10°$ respectively in steady and unsteady state at Mach number 0.4, inviscid fluid and turbulent flow. Air was selected as the fluid with the following specific properties ρ=1.164 kg/m^3 and ν= 1.57×10^{-5} m^2/s. The boundary conditions, all outer zones pressure are set to atmospheric Pressure. The contour map shows the pressure distribution on the upper and the lower surfaces of the wing. It has been shown the maximum value of pressure was found at the leading edge. Then, it has been shown when the attack angle increasing. The maximum value of pressure zone was tended to appear on the lower of airfoil surface as shown in figure (3). The pressure distribution was decreased after the leading edge and the section of the camber. This is due to increase in flow velocity and the angle of attack. At the trailing edge the pressure distribution was increased due to decrease in flow velocity and increasing the angles of attack.

Fig.5 points the relationship between the pressure distribution and the chord length of airfoil at attack angle= $0°$, steady and unsteady state condition. After the tip point of airfoil, the pressure value was fallen very quickly until the distance of 0.1 m. Then after the distance 0.2 m the response of pressure distribution was began to increase slowly as linear relation. While at the lower surface of airfoil was increased at higher value than the upper surface in length of chord= 0.1 m. Then, the pressure value was reached the same value at the length of chord =0.5 m. this is the point of trailing edge of airfoil.

Fig.6 describes the relation between the pressure distribution chord length at steady and unsteady state with angle of attack= $5°$. It has been shown the same response of relation of previous figures only a very little difference in values of pressure distribution.

Fig.7 illustrates the relation between the pressure distribution chord length at steady and unsteady state with angle of attack= $10°$. It has been noted in unsteady state the value of pressure at airfoil tip was a higher than the value in steady state. Also, from the results, it has been pointed that the pressure distribution on lower surface of airfoil increasing while pressure distribution decreasing on upper surface of airfoil when the attack angle was increased. These results were consistent with theoretical results of Petroski (2009).

Fig.8 describes the relationship between the pressure ratio and span length ratio. The maximum value of pressure ratio was found at the root of wing due to the maximum bending moment occurs at the root. The pressure ratio was decreased after the root of the wing and along the length of the span until reaching to the tip wing. At the tip wing the pressure ratio becomes zero. This is due to minimum bending moment was occurred at this location. These information's were detailed by Doherty [9]:

$$p(x) = p_r \sqrt{L^2 - x^2} \tag{8}$$

5.2 Stress Analysis

The structural analysis was achieved by using the ANSYS[11] package in order to obtain the element stresses distribution on the wing structure and the internal structure which included the ribs and spars along element coordinates axis, the linear and angular displacements of the nodes $(u, v, w, \theta_{xi}, \theta_{yi}, \theta_{zi})$ along global coordinate axis by using isotropic material.

Fig.9 points isometric view Von Misses stress contour distribution on the wing box. The maximum Von Misses stress occur at the distance of 0 to15% from the wing constraint or fixed edge at the root [$\sigma_{max} = 50.5$ MPa] which represented by red color due to maximum bending moment at this location.

Fig.10 represents Von Misses stress contour distribution on the internal structure of the wing box which includes the main spar (front spar), secondary spar (rear spar) and ribs. From figure noted that the higher values of Von Misses stress occurs at the distance of 0 to15% from the wing root which represented by red color due to maximum bending moment at this location.

Fig.11 describes vertical displacement field of the wing box (uy). From figure the maximum deflection occurs at the free side of the wing or at the tip ($(uy)_{max}$=1.25 cm), and the deflection is the inversely proportional with the stiffness values.

6. CONCLUSIONS

The major and general observations and conclusions for this work can be listed below:

1. From aerodynamic analysis results it can be noticed that the pressure value decrease in the upper surface with increase angle of attack due to changing the direction of flow and increasing in flow velocity, and the pressure value increase in the lower surface with increase angle of attack surface due to decrease in velocity of flow.

2. From the structural results it is noticed that the highest values of Von Misses stress occur at the distance of 0-15 % from the wing constraint or fixed edge at the root due to bending moment is maximum at this location.

3. The stress is also high at the corners at which spar webs extending from the wing and root rib intersects. The geometrical discontinuity is the reason for high stresses at these locations. So the designation is accepted.

4. Stress value on the spars is greater than the ribs and designed to have great bending strength. Ribs have minimum Von Misses stress due to bending moment carried by spars. Ribs designed to have great shear effect.

Table (1) aircraft wing geometric parameters. Ref. Unlusoy (2010)

Airfoil Section	NACA 4412
Plane form Area ,S	1.5[m^2]
Chord length ,C	0.5[m]
Wing span ,b	3[m]
Aspect Ratio ,A	6
Taper Ratio , λ	1
Thickness to Chord Ratio ,t/c	0.12

Table (2) Mechanical properties of aluminum 7075-T651 material, Ref. Unlusoy(2010).

Density, ρ	2810 [kg/m^3]
Young's modulus ,E	71.7[GPa]
Shear modulus ,G	26.9[GPa]
Poisson's ratio ,ν	0.33
Ultimate strength	572[MPa]
Yield strength	503[MPa]
Shear strength	331[MPa]

Table (3) element types for wing box structural members

Structural member	Element type
Spar webs	shell 281
Skin	shell 63
Ribs	shell 281

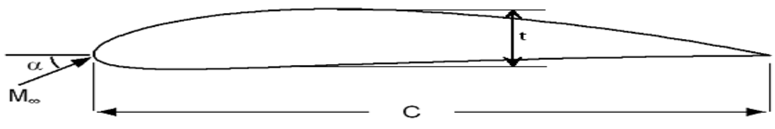

Figure (1) NACA 4412 airfoil. Ref. Petroski (2010)

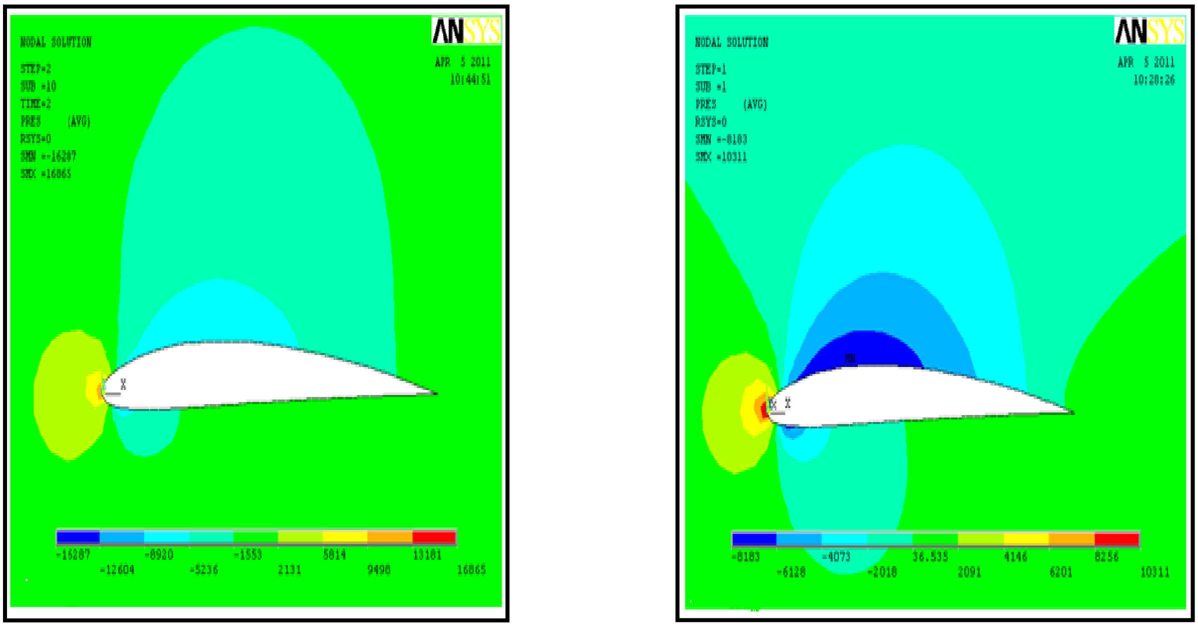

(a) steady state. (b) unsteady state.

Fig.2 contour map of pressure distribution across airfoil at $\alpha = 0^{\circ}$.

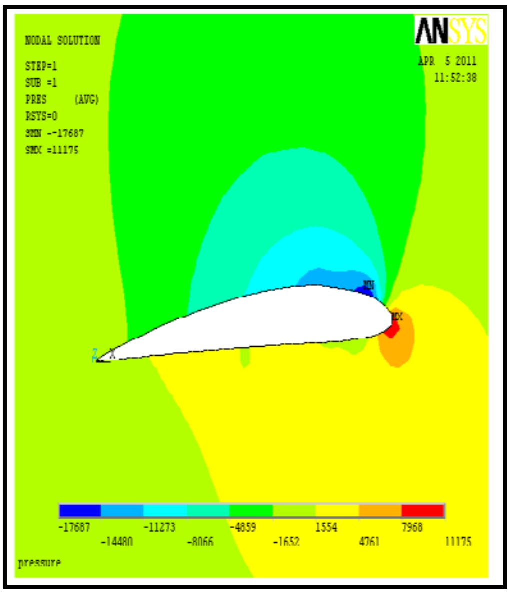

(a) steady state. (b) unsteady state.

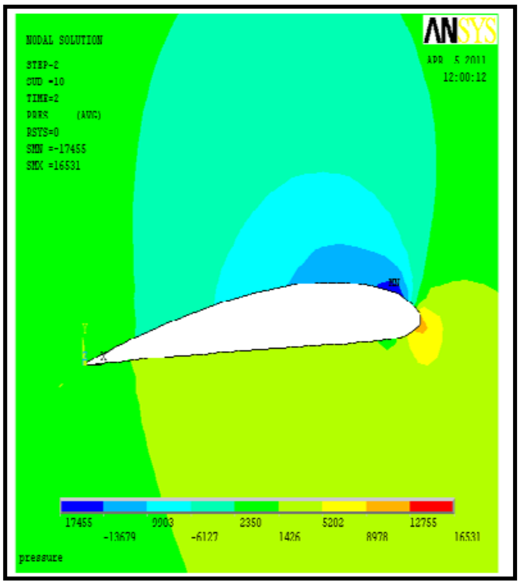

ig. 3 contour map of pressure distribution across airfoil at $\alpha = 5°$.

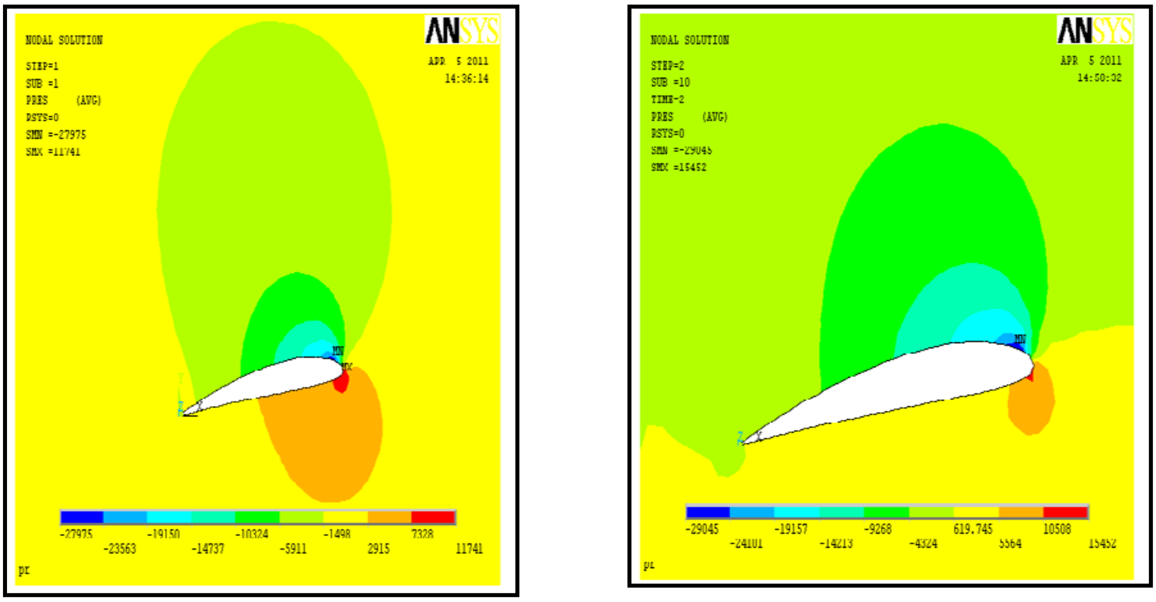

(a) steady state. (b)unsteady state.

Fig.4 contour map of pressure distribution across airfoil at $\alpha = 10°$.

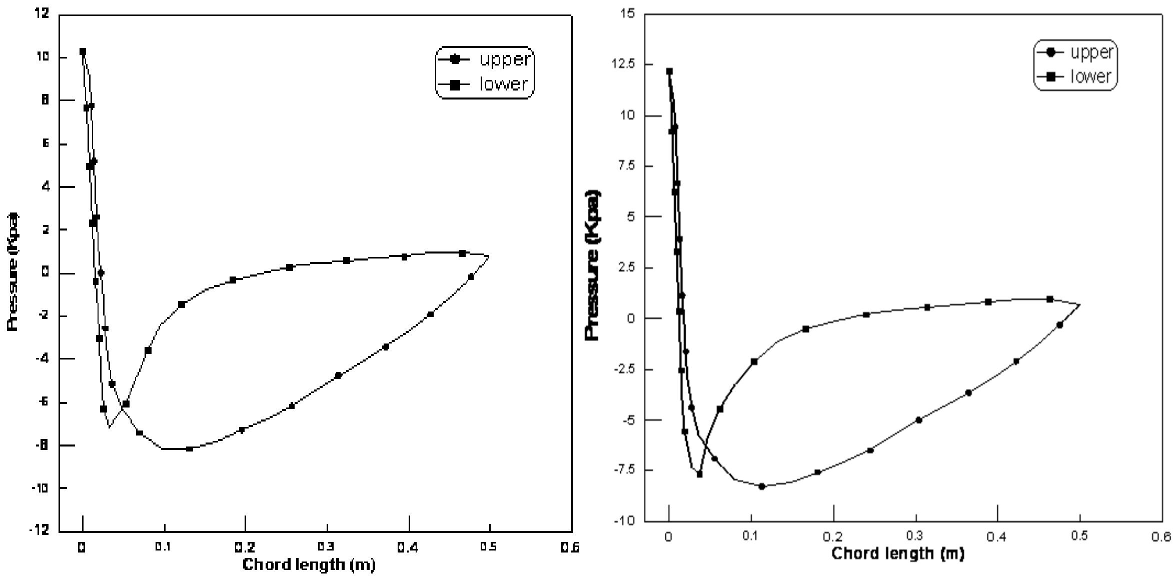

(a) steady state. (b)unsteady state.

Fig.5 pressure distribution across the airfoil at $\alpha = 0°$.

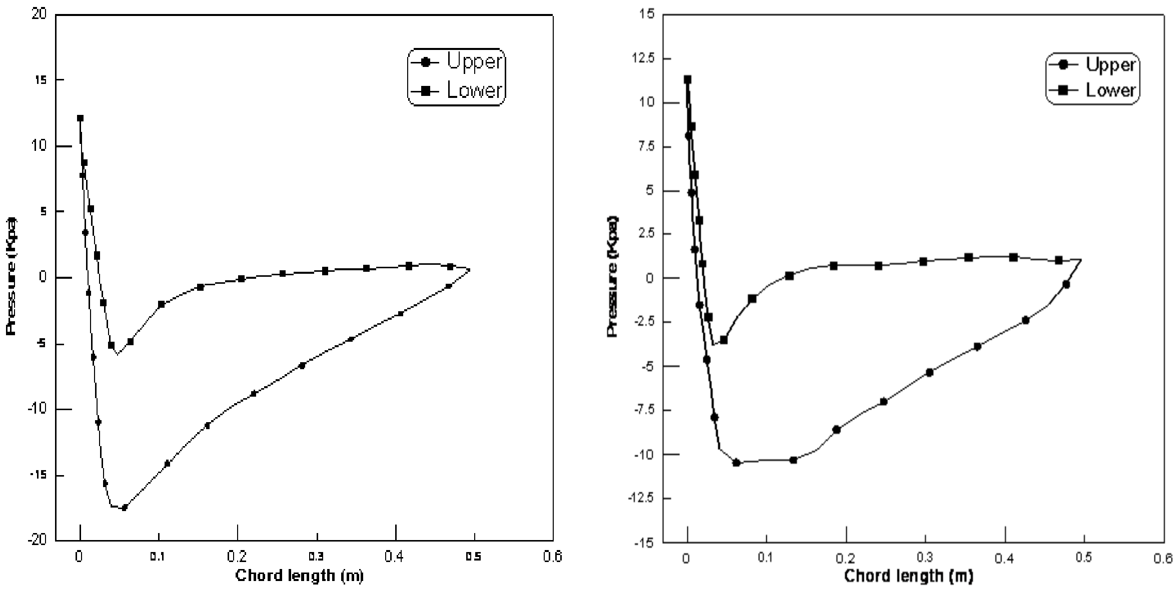

(a)steady state. (b) unsteady state.

Fig.6 pressure distribution across the airfoil at $\alpha = 5°$.

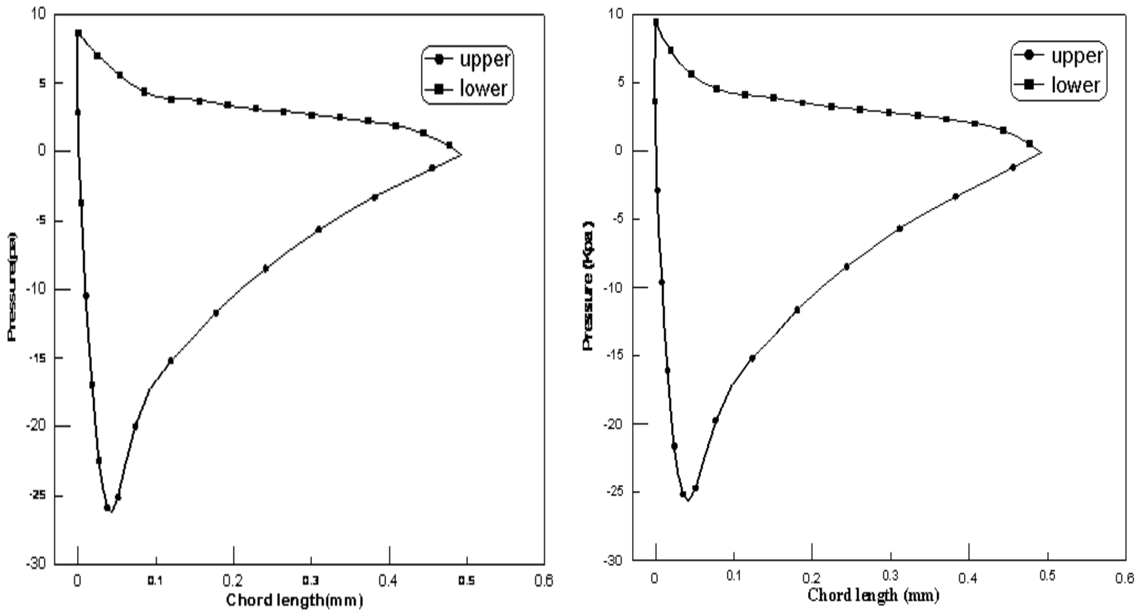

Fig.7 pressure distribution across the airfoil at $\alpha = 10^\circ$.

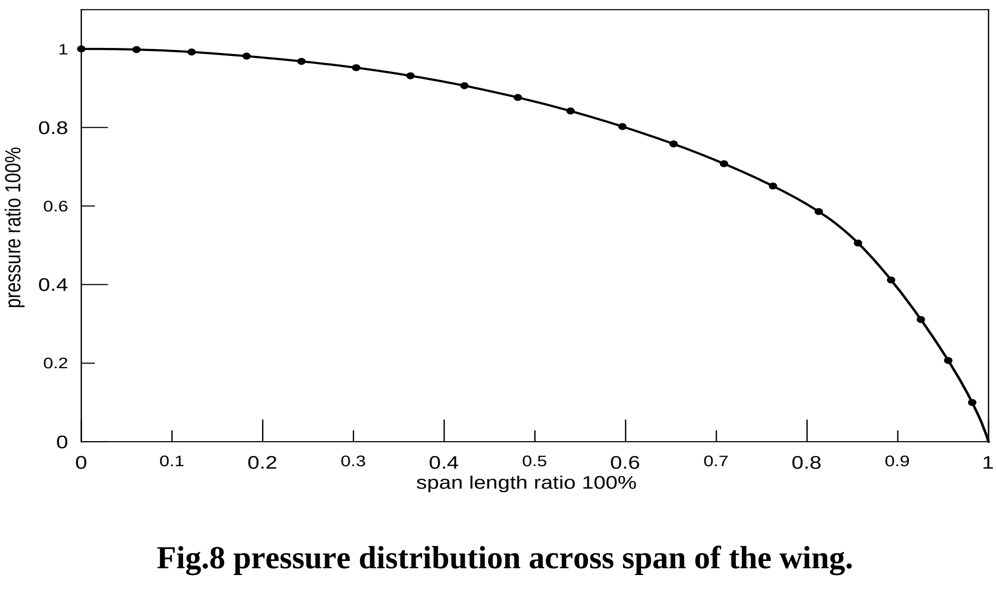

Fig.8 pressure distribution across span of the wing.

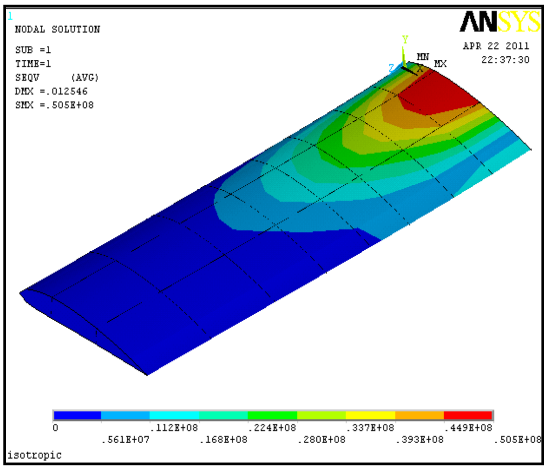

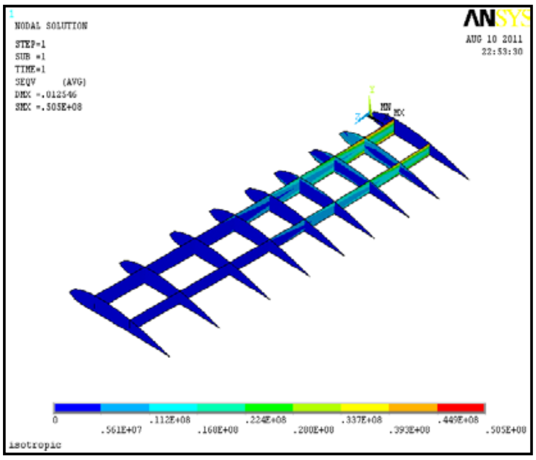

Fig.9 **Fig.10**

Fig.9 Von Misses stress distribution.
on the wing box
Fig.10 Von Misses stress distribution on the internal structure of the wing box.

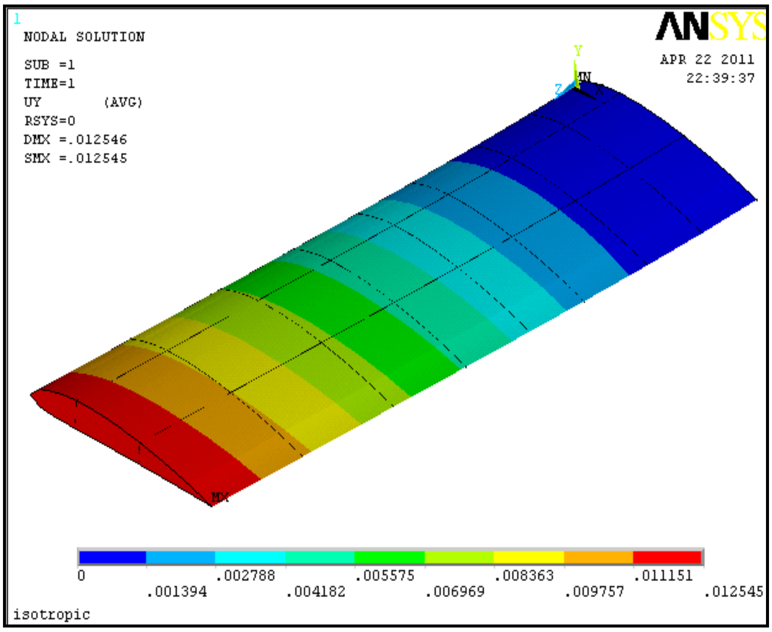

Fig.11 vertical displacement field on the wing box.

REFERENCES

Dan Doherty, 2008," Analytical Modeling of Aircraft Wing Loads Using Matlab and Symbolic Math Toolbox" , MSC thesis , department of mechanical engineering and aerospace engineering, West Verginia university, USA,1992.

Erdogan Tolga Insuyu, 2010," Aero-Structural Design and Analysis of an Unmanned Aerial Vehicle and its Mission Adaptive Wing", Aerospace Engineering, Middle East Technical University.

Henry Petroski, 2009," Applied Computational Aerodynamics", American Scientist, Vol. 82, Jan-Feb. 1994, pp.6-91997.Mechanical Engineering, University of Texas at Arlington.

Hansen and Hvejsel, 2007," Efficient finite element formulation for analysis and optimization of laminated composite shell structures" M.S.C thesis, Department of Mechanical Engineering, Aalborg University, Denmark.

Levent Unlusoy, 2010," Structural Design and Analysis of The Mission Adaptive Wings of an Unmanned Aerial Vehicle" Msc. thesis, Aerospace Engineering, Middle East Technical University.

Subbaraj.K., 1987,"A Survey of Direct Time Integration Methods in Computational Structural Dynamics-ii.Implicit Method",Computers and Structures, Vol.32, No.6, p.p. 1387-1410.

Salah H. Abid-Aun, 2008," Optimization of Light Weight Aircraft Wing Structure "Journal of Engineering and Development, Vol. 12, No. 1,Mechanical Engineering Departure, Institute of Technology, Baghdad, Iraq.

Sercan Soysal, 2008," Structural Design, Analysis and Composite Manufacturing Applications for a Tactical Unmanned Air Vehicle" Aerospace Engineering, Middle East Technical University.

Sakarya, Evren, 2010,"Structural Design and Evaluation of and Adaptive Camber Wing", MSc. Thesis, METU.

Zienkiewicz, O. C., and Newton, R. E., 1969, "Coupled Vibrations of a Structure Submerged in a Compressible Fluid", Proceedings of the Symposium on Finite Element Techniques, University of Stuttgart, Germany.